

Status of Multiphysics Modeling of Critical DPCs in a Geological Repository

Spent Fuel and Waste Disposition

***Prepared for
US Department of Energy
Spent Fuel and Waste Science and Technology***

***Mathew Swinney, Nithin Panicker, Nicholas Kucinski,
Aaron Wysocki, and Gregory Davidson
Oak Ridge National Laboratory***

***September 20, 2023
M3SF-23OR010305027
ORNL/SPR-2023/3123***

DISCLAIMER

This information was prepared as an account of work sponsored by an agency of the U.S. Government. Neither the U.S. Government nor any agency thereof, nor any of their employees, makes any warranty, expressed or implied, or assumes any legal liability or responsibility for the accuracy, completeness, or usefulness, of any information, apparatus, product, or process disclosed, or represents that its use would not infringe privately owned rights. References herein to any specific commercial product, process, or service by trade name, trademark, manufacturer, or otherwise, does not necessarily constitute or imply its endorsement, recommendation, or favoring by the U.S. Government or any agency thereof. The views and opinions of authors expressed herein do not necessarily state or reflect those of the U.S. Government or any agency thereof.

Replace by RES attachment

ACKNOWLEDGMENTS

This research was sponsored by the Spent Fuel and Waste Science and Technology Program of the US Department of Energy and was carried out at Oak Ridge National Laboratory under contract DE-AC05-00OR22725 with UT-Battelle LLC. This research used resources of the Compute and Data Environment for Science (CADES) at the Oak Ridge National Laboratory, which is supported by the Office of Science of the US Department of Energy. The authors would like to thank Emilian Popov for the technical advice he provided.

This page is intentionally left blank.

SUMMARY

This report documents work performed in support of the US Department of Energy (DOE) Nuclear Energy Spent Fuel and Waste Disposition (SFWD) Spent Fuel and Waste Science and Technology under work breakdown structure element 1.08.01.03.05, “Direct Disposal of Dual Purpose Canisters.” In particular, this report fulfills M3 milestone M3SF-23OR010305027, "Multiphysics modeling of DPCs" within work package SF-23OR01030507, “DPC Criticality Modeling and Support — ORNL.”

This report details ongoing work in the development of multiphysics modeling and simulation techniques for critical dual-purpose canisters (DPCs) in a saturated repository. The analysis has focused on four scenarios: (1) partially flooded critical DPCs in which the excess reactivity is low enough that the water remains subcooled, (2) fully flooded subcooled critical DPCs, (3) partially and fully flooded critical DPCs in which the excess reactivity is great enough to cause the water to boil, and (4) DPCs that are sealed in by the surrounding bentonite backfill to the extent that high pressures can be achieved.

A summary of previous work focused on the first two scenarios is presented as an established workflow. These canisters could reach an equilibrium at a low quasi-steady-state power level that could be sustained for thousands of years. The majority of this report describes an effort to expand the initial methodology to include the scenario in which a DPC has enough excess reactivity to boil the water inside the canister. This scenario involves a variety of tools and modeling approaches to capture the two-phase behavior, including RELAP5-3D, STAR-CCM+, and TRACE. Efforts using the high-fidelity computational fluid dynamics results to verify the accuracy of RELAP5-3D and TRACE for boiling DPCs are also presented. A new modeling strategy using TRACE appears to be the most promising approach for expanding the analysis of critical DPCs beyond the subcooled scenarios. Finally, this report describes ongoing work investigating the fourth scenario, in which a critical DPC is sealed in saturated bentonite. The primary goal in this research is to understand the power output and associated pressure increase to inform geomechanics simulations that could predict the impact on a geological repository.

This page is intentionally left blank.

CONTENTS

LIST OF FIGURES **viii**
LIST OF TABLES **ix**
ACRONYMS **x**
1. Introduction **1**
2. Critical Subcooled DPCs **3**
 2.1 Simulation Codes 3
 2.2 Subcooled Partially Flooded DPC Example 4
 2.3 Subcooled Fully Flooded DPC Workflow 5
3. Evaluating TH tools for boiling canisters **10**
 3.1 Motivation 10
 3.2 FY22 Full-Scale Dual-Purpose Canister Model 11
 3.3 Full-Scale Dual-Purpose Canister Vertical Pipe Model 13
 3.4 Simple boiling test case 17
 3.5 2D Canister Modeling with TRACE 19
 3.6 Planned verification work 24
4. DPCs sealed in a Bentonite backfill **27**
5. Conclusions and Future Work **30**

LIST OF FIGURES

1	Workflow for estimating the quasi-static power level in a specific DPC and generating the corresponding nuclide inventory.	6
2	Coupling of physics simulation codes for power and radionuclide inventory calculations. . .	7
3	Example of a critical moderator density search for three reactive MPC-32 DPCs.	8
4	Comparison of radioactive fission product densities in the multipurpose canister (MPC)-32-162 model with and without a 10,000 year criticality event producing 2.47 kW.	10
5	Side-view of the three-ring setup used in the FY22 reactor excursion and leak analysis program 5 - three dimensional (RELAP5-3D) MPC model.	12
6	Component diagram for the FY22 RELAP5-3D MPC model.	12
7	Vertical pipe setup used in RELAP5-3D DPC model.	13
8	Heat structure grouping scheme used in RELAP5-3D MPC model.	13
9	Full-scale DPC RELAP5-3D model.	14
10	Geometries considered for CFD modeling: previous (left) and current (right).	15
11	Mesh on a plane cutting the fuel rods.	16
12	Simple boiling test case RELAP5-3D model.	17
13	Simple boiling test case RELAP5-3D model.	18
14	Volume fraction of bubbles on a cut-section of the geometry.	19
15	Representation of test problem (not to scale): trac/relap advanced computational engine (TRACE) (left) and CFD (right).	21
16	Test problem TRACE model.	21
17	Vessel cell refinement schemes used in TRACE test problem.	23
18	Temperature contour predicted by CFD on a cut section.	23
19	Natural circulation contour predicted by Simulation of Turbulent flow in Arbitrary Regions – Computational Continuum Mechanics (STAR-CCM+) on a cut section.	24
20	Down-scaled canister model.	26
21	A depiction conceptualizing a DPC in a drift back-filled with bentonite.	27
22	An example of the results from the new workflow predicting k_{eff} in a sealed DPC as a function of power. The temperatures listed on the plot represent the peak fuel temperatures in the model.	29
23	Pressure buildup in a sealed DPC as predicted with RELAP5-3D at a power level of 5 MW. .	29

LIST OF TABLES

1	Critical water level in MPC-32-TSC 079 (Sequoyah Independent Spent Fuel Storage Installation (ISFSI)	5
2	Steady-state power estimates for two MPC-32 DPCs using the established workflow.	9
3	Dimensions and initial conditions for an MPC-32 boiling case.	15
4	Predicted fluid properties for fullScale MPC-32	16
5	Predicted liquid mass loss comparison for full-scale MPC-32	17
6	Dimensions and initial conditions for simple boiling case	18
7	Predicted liquid mass loss comparison for simple boiling cases	19
8	Dimensions and initial conditions for TRACE test problem	22
9	Axial power profile used in TRACE test problem	22
10	Cell temperatures in the TRACE cases and the Star-CCM+ case for the 2D problem	25
11	Wall heat loss in the TRACE cases and the Star-CCM+ case for the 2D problem	25
12	Example temperature profile for sealed DPC (500 kW case)	28

ACRONYMS

CADES	Compute and Data Environment for Science
CFD	computational fluid dynamics
DOE	U.S. Department of Energy
DPC	dual-purpose canister
LBNL	Lawrence Berkeley National Laboratory
LWR	light water reactor
MC	Monte Carlo
MPC	multipurpose canister
ORNL	Oak Ridge National Laboratory
RELAP5-3D	reactor excursion and leak analysis program 5 - three dimensional
SFWD	Spent Fuel and Waste Disposition
SNF	spent nuclear fuel
STAR-CCM+	Simulation of Turbulent flow in Arbitrary Regions – Computational Continuum Mechanics
TH	thermohydraulics
TOUGH	Transport Of Unsaturated Groundwater and Heat
TRACE	trac/relap advanced computational engine

1. INTRODUCTION

This report documents work performed in support of the U.S. Department of Energy (DOE) Nuclear Energy Spent Fuel and Waste Disposition (SFWD) Spent Fuel and Waste Science and Technology under work breakdown structure element 1.08.01.03.05, “Direct Disposal of Dual Purpose Canisters.” In particular, this report fulfills M3 milestone M3SF-23ORXXXX, “Multiphysics criticality consequence analysis FY23 Milestone Report” within work package SF-23ORXXXX, “DPC Reactivity and Criticality Modeling — ORNL.”

DPCs are designed for the storage and transportation of spent nuclear fuel (SNF), but DPCs have not been approved for permanent disposal in a future geological repository [1]. If they are disposed in a saturated repository, then some DPCs may fail and flood under the conditions and timescales associated with long-term disposal. Once this occurs, most of the neutron absorber elements preventing criticality may corrode and fail, thus allowing some DPCs to achieve criticality. In response to these concerns, an Oak Ridge National Laboratory (ORNL) research team is developing a multiphysics simulation workflow to support investigations into the potential consequences of criticality in as-loaded DPCs in a saturated repository. Four hypothetical scenarios have been identified thus far, each requiring different strategies to quantify the associated consequences. Each case considers a critical DPC that has lost all the neutron absorbers designed to prevent criticality. These scenarios are summarized below.

Scenario 1: Partially flooded, subcooled DPC

This scenario concerns DPCs that are partially flooded with water. The quantity of interest in this modeling scenario is the water level necessary to sustain criticality for a given DPC. This can inform the time-to-criticality after a DPC has been breached.

Scenario 2: Fully flooded, subcooled DPC

This scenario assumes that a DPC is fully flooded with water but that the excess criticality is not great enough to boil the water. The quantities of interest are the maximum sustainable power level and the resultant time-dependent isotopic inventory, providing a source term for repository-scale analysis.

Scenario 3: Boiling water within a DPC

When a critical DPC has a sufficiently large amount of excess reactivity, the water within the DPC will become hot enough to boil. In this scenario, two-phase thermohydraulic modeling is necessary to correctly capture the temperature and power distribution within the DPC. Quantities of interest include power distribution and isotopic inventory, providing a source term for repository-scale analysis.

Scenario 4: DPC sealed within the bentonite backfill

The bentonite backfill within a drift becomes saturated with water over time and swells. Because the bentonite is highly water impermeable, this effectively seals up the DPC such that water cannot escape within timescales relevant to a criticality excursion. This scenario is likened to a “pressure cooker.” Pressures and associated temperatures and power levels within the DPC could become large enough so that fracturing of the bentonite is the only relief mechanism. Quantities of interest are power levels and DPC pressure, which provide inputs to geomechanics analysis. The realistic feasibility of this scenario is still being evaluated.

This report continues and expands upon the work documented in Swinney et al. [2, 3], in which a method for computing the sustainable power level of a critical DPC is presented. Previous work focused on cases in which the DPC is only partially filled (Scenario 1) or completely flooded but remains subcooled

42 (Scenario 2). Both of these cases and the associated methodologies are summarized in Section 2. Recent
43 efforts have focused on extending the analysis to the remaining two scenarios, which will require notably
44 different tools and modeling strategies.

45 Progress toward modeling Scenario 3 will be presented in Section 3. This case describes a configuration
46 in which there is enough excess reactivity within a flooded DPC to not only achieve criticality, but to achieve
47 it at a power level that causes boiling within the canister. Previous modeling could not capture this two-phase
48 behavior, and developing a methodology to properly simulate this phenomena has been the primary focus
49 of this year's efforts.

50 The efforts to understand Scenario 4 are presented in Section 4. This case describes a theoretical
51 situation in which water can slowly enter the waste package through the bentonite backfill, but once the
52 DPC is fully flooded and the neutron absorbers have been lost, water cannot escape once criticality begins.
53 This situation is considered plausible because of the incredibly low permeability of the bentonite backfill.
54 Water will migrate through the clay over hundreds or thousands of years, but once criticality begins, the
55 bentonite will be relatively impermeable on the short timescale during which criticality occurs. Analysis
56 of this scenario also required the development of new tools and strategies with the primary purpose of
57 understanding the achievable power levels and associated pressure rise within a sealed DPC. Ultimately,
58 geomechanics calculations will be necessary to understand how a repository would behave under these
59 conditions. This effort, like the work described in Section 3 is currently in progress.

60 Moving forward, the capabilities being developed for modeling boiling and sealed DPCs will be imper-
61 ative for expanding the analysis of critical DPCs beyond those in the quasi-static subcooled regime. Section
62 5 discusses the direction of future work for the analysis of critical DPCs in a saturated repository with a fo-
63 cus on canisters and conditions not well captured by the existing methodology and capabilities. Ultimately,
64 this effort will inform a more comprehensive understanding of the potential consequences of a critical DPC
65 in a saturated repository.

2. CRITICAL SUBCOOLED DPCS

66

67 The work preceding this year's efforts focused on developing a methodology to estimate the quasi-
68 static power level of subcooled critical DPCs in a saturated repository using loosely coupled multiphysics
69 simulations [4]. This method used a variety of tools, including the UNF-ST&DARDS software and the
70 associated database for creating as-loaded DPC models [5], the SCALE 6.3 code package, including the
71 Shift Monte Carlo code for criticality calculations [6], ORIGEN for isotopic depletion [7], RELAP5-3D for
72 in-canister thermal hydraulics [8], and PFLOTRAN for repository thermal hydraulics [9]. A brief overview
73 of the current state of the workflow is presented in Section 2.3.1. For a more complete description, refer to
74 previous works [2, 3].

75 Additional work last year [3] addressed the investigation into the effect of moderator density on reac-
76 tivity in various DPC types. Moderator density has been shown to be the primary factor for determining
77 the power level for a fully flooded, subcooled DPC in the quasi-static regime. This effect was characterized
78 for various DPC designs supported by calculations using specific as-loaded DPCs. These data can be used
79 to predict the quasi-static power level within any DPC without the need to perform simulations for each
80 canister. This demonstrates the primary strategy for extending the current methodology to include a large
81 portion of the current US inventory of SNF awaiting disposal. An additional parameter studied in this effort
82 was the effect of criticality start time, which was varied from immediately upon disposal to up to 500,000
83 years post closure.

84 Section 2.1 discusses the various simulation codes used to perform analysis of subcooled critical DPCs.
85 Section 2.2 discusses Scenario 1 and the method used to compute the critical water level in a partially filled
86 DPC. Section 2.3 summarizes the methodology for calculating power in a critical fully flooded subcooled
87 DPC, and it also presents some examples.

2.1 SIMULATION CODES

88

89 Three simulation codes are utilized to compute the sustainable power level in a critical DPC. Each
90 simulation code is described briefly below.

2.1.1 SHIFT-ORIGEN RADIATION TRANSPORT AND DEPLETION CODE

91

92 Shift is a general-purpose high-performance massively parallel Monte Carlo (MC) code featuring continuous-
93 energy and multigroup physics. Shift is capable of solving problems in both k -eigenvalue and fixed-source
94 modes [6], and it can model coupled neutron/photon physics, including secondary particles born both
95 through inelastic scattering and fission. Shift is also fully coupled to the automatic cross-section generation
96 capabilities in the SCALE code package [10]. Shift has been previously used for SNF analysis, including
97 radiation dose calculations [11].

98 Shift also features a depletion package with full coupling to ORIGEN [7]. ORIGEN is a general-
99 purpose nuclide depletion code featuring nuclide activation, depletion, and decay. Shift has a series of high-
100 fidelity depletion coupling algorithms [12], including algorithms specifically designed for constant-power
101 depletion of the same type used in the analysis of critical DPCs [13].

2.1.2 RELAP5-3D THERMOHYDRAULICS CODE

102

103 RELAP5-3D [8] is a standard system analysis simulation code developed by Idaho National Labora-
104 tory. This code was developed to analyze steady-state and transient thermohydraulics (TH) behavior in
105 light water reactors (LWRs). It is a best-estimate code developed for transient simulations of LWR coolant

106 systems during operational transients and postulated accident scenarios, and it can be used for modeling
107 other nuclear and non-nuclear systems. RELAP5-3D has a fully integrated, multidimensional TH and ki-
108 netic modeling capability, making it applicable to a wide range of systems and applications. The code is
109 extensively validated [14, 15] and widely accepted in the nuclear industry for systems analysis applications.
110 The code can be used to simulate a wide variety of thermal transients in nuclear and non-nuclear systems
111 that involve mixtures of vapor, liquid, noncondensable gas, and nonvolatile solute.

112 RELAP5-3D is a systems-level analysis code and is not intended for channel-by-channel TH solu-
113 tions. A subchannel solver designed for this purpose would provide a higher fidelity TH solution. COBRA-
114 SFS [16] is a single-phase subchannel code often used to analyze spent fuel canisters filled with air. Unfor-
115 tunately, there is not much validation work available for COBRA-SFS using water. A two-phase subchannel
116 code capable of simulating partially filled or boiling DPCs would provide a higher level of fidelity and would
117 enable the simulation of a variety of canister configurations. Because of the limitations in COBRA-SFS,
118 RELAP5-3D was used to simulate the TH properties within a critical, subcooled DPC instead. This tool
119 proved to be sufficient for these scenarios.

120 2.1.3 PFLOTRAN REPOSITORY-LEVEL THERMOHYDRAULICS CODE

121 PFLOTRAN is a 3D massively parallel multiphase flow and reactive transport simulator for modeling
122 subsurface processes [9]. It is open source and freely available, and it is primarily developed by Sandia
123 National Laboratories and Pacific Northwest National Laboratory for the DOE Spent Fuel Waste Science and
124 Technology program. PFLOTRAN is primarily used for large-scale probabilistic performance assessment
125 simulations to constrain the fate of radioactive contaminants over the performance period of a geologic
126 radioactive waste repository.

127 In PFLOTRAN, the flow and energy transport equations are solved separately from solute transport, and
128 then they are sequentially coupled. In the GENERAL flow mode, a system of three partial differential equa-
129 tions describing two-phase two-component flow coupled with energy transport are solved fully implicitly to
130 obtain distributions of pressure, temperature, and phase saturation everywhere in the domain. The Global
131 Implicit Reactive Transport mode then solves solute transport at either the same time step or at a smaller
132 time step than flow. The two modes sync at the flow time step and exchange relevant state variables. Gen-
133 erally, this sequential coupling is robust for large time steps because trace solute concentrations are linearly
134 independent from flow variables such as density and temperature. If there is significant interaction between
135 the state variables of flow and transport, then the simulator will likely take small time steps, which could
136 be prohibitive. The final result is repository-wide coupled two-phase flow; heat transfer; and radionuclide
137 transport, decay, ingrowth, and sorption.

138 2.2 SUBCOOLED PARTIALLY FLOODED DPC EXAMPLE

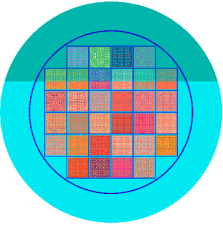
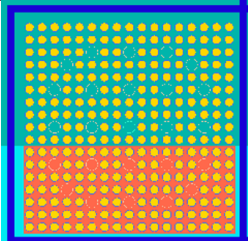
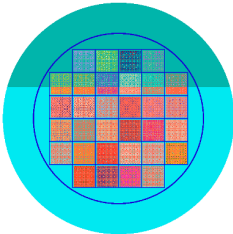
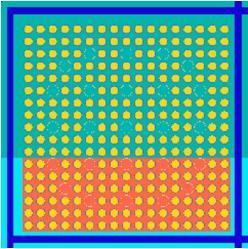
139 The first critical DPC scenario investigated was the subcooled, partially flooded DPC. This work in-
140 volved simulations attempting to capture a slowly flooding DPC that had lost the internal neutron absorbers.
141 To gain insight into critical configurations for typical SNF canisters, a series of criticality calculations was
142 performed using Shift to determine the critical water level for a realistic MPC-32-TSC canister. The ra-
143 diation transport models were generated with UNF-ST&DARDS, which uses operational data to build as-
144 loaded casks with used fuel assemblies.

145 All of the canisters generated with the UNF-ST&DARDS tool are completely submerged in water and
146 required modification to simulate a canister that was only partially filled. This was a nontrivial task that
147 required substantial analysis effort. The final workflow essentially entailed duplicating the model, replacing
148 the water with air everywhere within the DPC, and manually modifying a geometry cutting plane that would

149 use the air model above the plane. One limitation of this methodology was that the water level could only
 150 be set at pin boundaries, so the water level could only be set to discrete values between individual layers of
 151 pins. Although the water level could not be set to an arbitrary value with this method, the level of fidelity
 152 (~1 cm) was sufficient for the level of analysis needed.

153 Once the models were generated, a simple criticality search was conducted to narrow down the precise
 154 water level that yielded a multiplication factor nearest to unity. The final result is illustrated in Table 1,
 155 which shows the two bounding cases that narrowed down the critical water level for the Sequoyah MPC-
 156 32-TSC-079 canister. Note that a similar analysis could be performed for any potentially critical canister.
 157 For this particular canister, the critical water level was approximately 103 cm from the bottom of the first
 158 row of assemblies. This information could be used to predict time to criticality once the canister has been
 159 breached.

Table 1. Critical water level in MPC-32-TSC 079 (Sequoyah Independent Spent Fuel Storage Installation (ISFSI))

Canister cross-section	Water level	Assembly cross section	Multiplication factor, k_{eff}
	~103.6 cm		1.00016506 ± 6
	~102.4 cm		0.994745 ± 5

160 2.3 SUBCOOLED FULLY FLOODED DPC WORKFLOW

161 The fidelity required by each of the three simulation codes necessitates different levels of model fidelity
 162 ranging from high-fidelity models for the Shift radiation transport code to lower fidelity models for the
 163 RELAP5-3D system-level thermohydraulics code. The DPC models used by Shift and RELAP5-3D have
 164 not fundamentally changed and are well described in the previous version of this report [2].

165 The current methodology still assumes a completely flooded canister at a constant pressure of 50 bars
 166 with all the neutron absorbers removed. For cases in which the absorbers are in plates, this entails replacing
 167 those volumes with water. For DPCs in which the absorbers are contained within the basket structure itself,
 168 the grid is removed, and the basket cells containing the assemblies in water are shifted toward the center of
 169 the DPCs.

170 Initially, power shapes generated by Shift were used to compute TH properties with RELAP5-3D, but it
 171 was observed that the fluid within the DPCs had a uniform density and temperature profile as a result of the
 172 flow mixing. Therefore, a single value for fluid temperature and corresponding fluid density was sufficient
 173 for use in the neutronics calculations. Justification for this treatment has been adequately documented in

174 previous work [3]. These TH properties were also used to verify the PFLOTRAN TH property predictions at
 175 various DPC power levels. This conclusion serves to justify the use of the TH fluid properties provided by the
 176 PFLOTRAN repository model data which were verified with the in-canister TH RELAP5-3D calculations.
 177 The result is the following simplified workflow for calculating the quasi-static power level in a DPC:

- 178 1. Calculate k_{eff} for a set of predefined TH state-points using the Shift DPC model.
- 179 2. Interpolate the critical moderator density from the resulting criticality data.
- 180 3. Use the predicted critical moderator density to interpolate the critical power level using the PFLO-
 181 TRAN proxy data.

182 Figure 1 represents the current workflow in practice, beginning with the initial stage of choosing a
 183 specific DPC to simulate to the final generation of nuclide inventory in the canister as a function of time
 184 and power generation. Despite the streamlined workflow, this methodology is still too time intensive to
 185 implement on every single DPC of interest in the current US inventory. This limitation was the basis for the
 186 work focused on expanding the methodology documented last year [3].

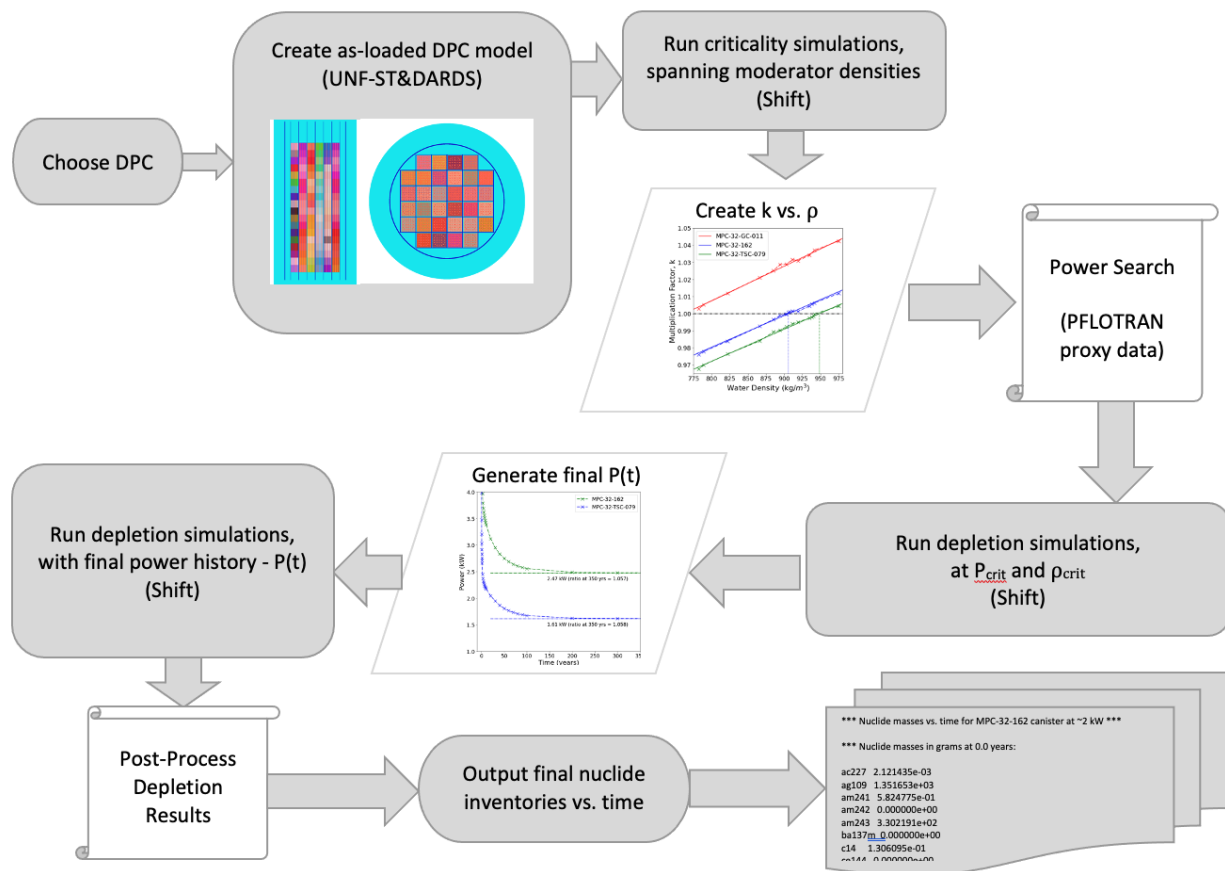


Figure 1. Workflow for estimating the quasi-static power level in a specific DPC and generating the corresponding nuclide inventory.

2.3.1 OVERVIEW OF WORKFLOW FOR CALCULATING POWER IN A CRITICAL DPC

189 Figure 2 illustrates the current physics coupling between the radiation transport (Shift), in-canister TH
 190 (RELAP5-3D), and the repository porous media (PFLOTRAN) solvers. Coupled together, these components

enable the calculation of the quasi-static power level in a critical DPC.

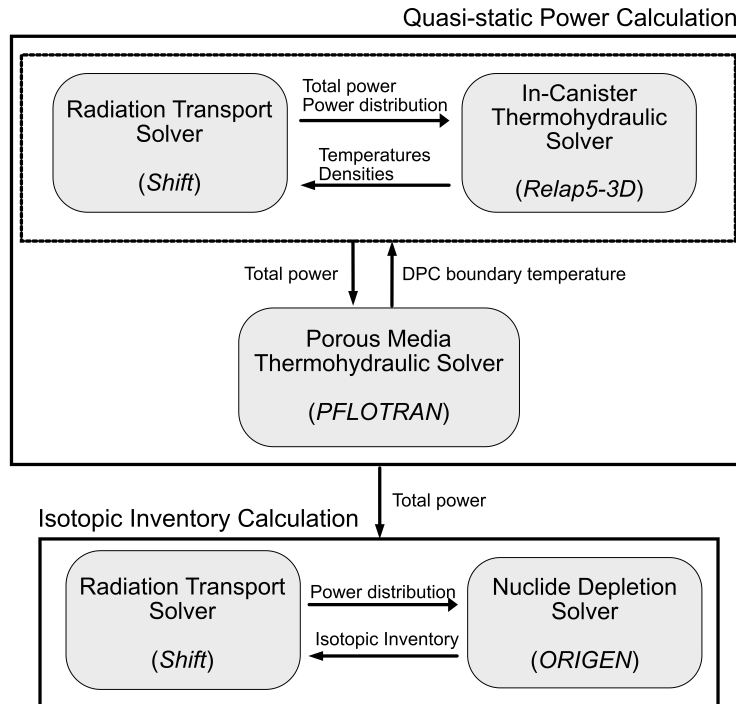


Figure 2. Coupling of physics simulation codes for power and radionuclide inventory calculations.

191

192 Because of the low power levels in critical DPCs (below 4 kW), the couplings between the various
 193 physics components are loose and nearly linear. Therefore, tight coupling in a full-fidelity multiphysics
 194 simulation is unnecessary. Instead, coupling is achieved through physics proxies or precomputed “lookup”
 195 tables of results that can be linearly interpolated and iterated to convergence. Thus, the method for comput-
 196 ing the power level and radionuclide inventory in a critical DPC is as follows:

- 197 1. Use the physics packages mentioned above and described in Section 2.1 to precompute proxy data
 198 spanning the plausible operating envelope of a critical DPC in a saturated repository.
- 199 2. Perform the inner and outer iterations by interpolating over the precomputed proxy data as illustrated
 200 in Figure 2 to compute the critical power level.
- 201 3. Use the critical power level to perform a radiation transport/nuclide depletion simulation to compute
 202 isotopic inventory as a function of time.

203 2.3.2 SUBCOOLED FULLY FLOODED DPC EXAMPLE

204 Although the partially flooded example described in Section 2.2 only utilized parts of the workflow
 205 described in Section 2.3.1 (UNF-ST&DARDS and Shift), the example presented here used the full workflow
 206 as prescribed. The methodology for computing the quasi-static power level in a DPC assumes that the fuel
 207 rods, in-canister water, and surrounding rock are all in thermal equilibrium. In this example, three reactive
 208 MPC-32 canisters were selected from the UNF-ST&DARDS database.

209 A geological repository model was employed to explore the plausible combinations of DPC power and
 210 boundary temperatures for a realistic repository environment. The PFLOTRAN repository model was set
 211 in saturated shale host rock at a depth of 500 m, with several different DPC power levels (1, 2, 4, and

212 6 kW). These were chosen to span the location where DPCs are expected to be capable of reaching a steady-
 213 state condition without boiling the water inside the DPC. Proxy data were then generated for each of these
 214 conditions, including TH state points within the waste package as a function of time, ultimately resulting
 215 in thermal equilibrium between the DPC and the repository for each power level. These data were then
 216 combined with critical moderator density curves generated with Shift calculations to enable a steady-state
 217 power estimate via interpolation. The critical moderator search showing Shift results is illustrated in Figure
 218 3.

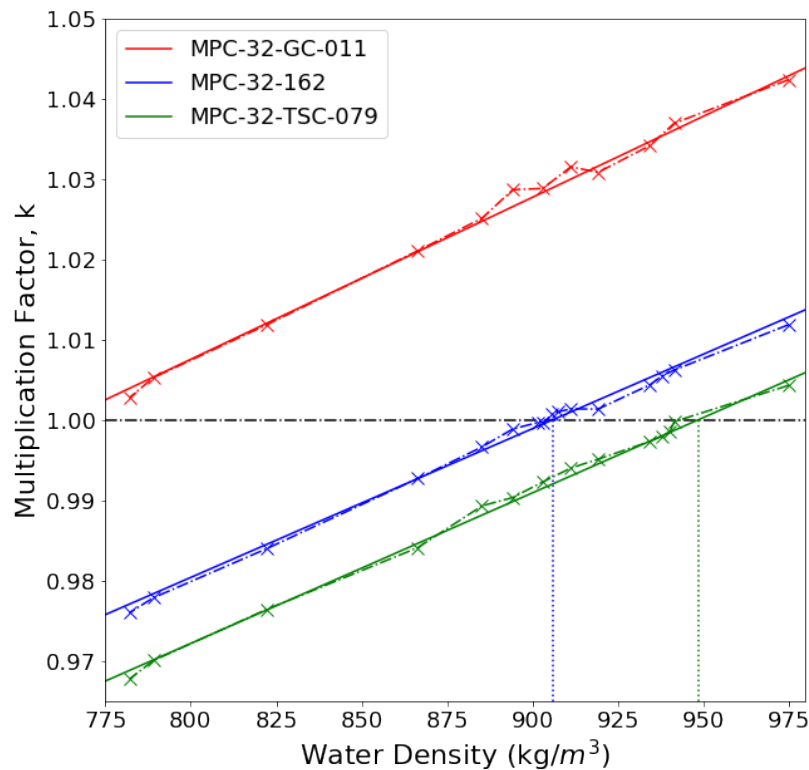


Figure 3. Example of a critical moderator density search for three reactive MPC-32 DPCs.

219 The results from the PFLOTRAN calculations yielded 3 steady-state power levels at 1, 2, and 4 kW with
 220 their associated canister boundary temperatures. To ensure that the two TH models agreed, the RELAP5-3D
 221 model was run again with these parameters and was shown to produce nearly identical fluid temperatures and
 222 densities at these power levels. These three PFLOTRAN state points were used to interpolate the converged
 223 critical power levels for the two example DPCs. As a final check, the two cases were run again using Shift,
 224 thus confirming that a k_{eff} of near unity was predicted for the MPC-32-162 canister (1.00077 ± 0.00022)
 225 and the MPC-32-TSC-079 canister (1.00049 ± 0.00021) given the stated fluid properties. The final canister
 226 shown (MPC-32-GC-011) remained critical, even when the moderator density reached the boiling point of
 227 water at 50 bars (near 776 kg/m^3). This methodology was therefore insufficient for this canister, illustrating
 228 the need for the work presented in Section 3.

229 A depletion analysis was also completed for the MPC-32-162 canister using the integrated radiation
 230 transport/depletion capabilities found in Shift/ORIGEN. The power shown in Table 2 was used to predict
 231 the isotopic inventory as a function of time resulting from the postulated criticality. The MPC-32-162 model
 232 created with the UNF-ST&DARDS software included a 20,000 year decay step, which was followed by a
 233 10,000 year steady-state criticality event described in the Shift input. This 20,000 year decay step represents

Table 2. Steady-state power estimates for two MPC-32 DPCs using the established workflow.

Boundary temp. (K)	Power (kW)	Moderator density (kg/m ³)	Fluid temp. (K)
Farley MPC-32-162 converged case			
436	2.44	905.93	437.22
Sequoyah MPC-32-TSC-079 converged case			
387	1.54	948.17	389.52

234 the time allowed for the canister to fail and flood, but it also represents another conservative worst-case
 235 assumption because this time frame has been shown to cover when the multiplication factor within the
 236 canister reaches a maximum [17]. A base case with no criticality (i.e., no power) was also simulated to
 237 serve as a comparison to the 2.47 kW criticality case.

238 Figure 4 illustrates the expected concentrations of some key radioactive fission and activation products
 239 that may be of concern for determining the consequences of the criticality to a member of the public. The
 240 inventory of short-lived fission products is predictably impacted because most of the pre-existing inventory
 241 has decayed away; therefore, the criticality generates a small inventory of short-lived fission products that
 242 would otherwise not be present. This additional nuclide inventory could be relevant to the performance of a
 243 repository, but the impact would likely be mitigated by the relatively quick decay of most of these nuclides
 244 as they are transported slowly to the boundary of the repository. Some of the nuclides that may be of interest
 245 include ¹⁵¹Sm (half-life ~90 yr), ⁹⁰Sr (half-life ~30 yr), and ¹³⁷Cs (half-life ~30 yr). Some of the actinides
 246 fall into a similar category, particularly ²⁴⁴Cm (half-life ~18 yr), ²³⁸Pu (half-life ~88 yr), and ²³²U (half-life
 247 ~69 yr). Most of the other “short-lived” nuclides have substantially shorter half-lives and should decay
 248 prior to leaving the repository. Results like these have been provided as the source term for repository-scale
 249 analysis.

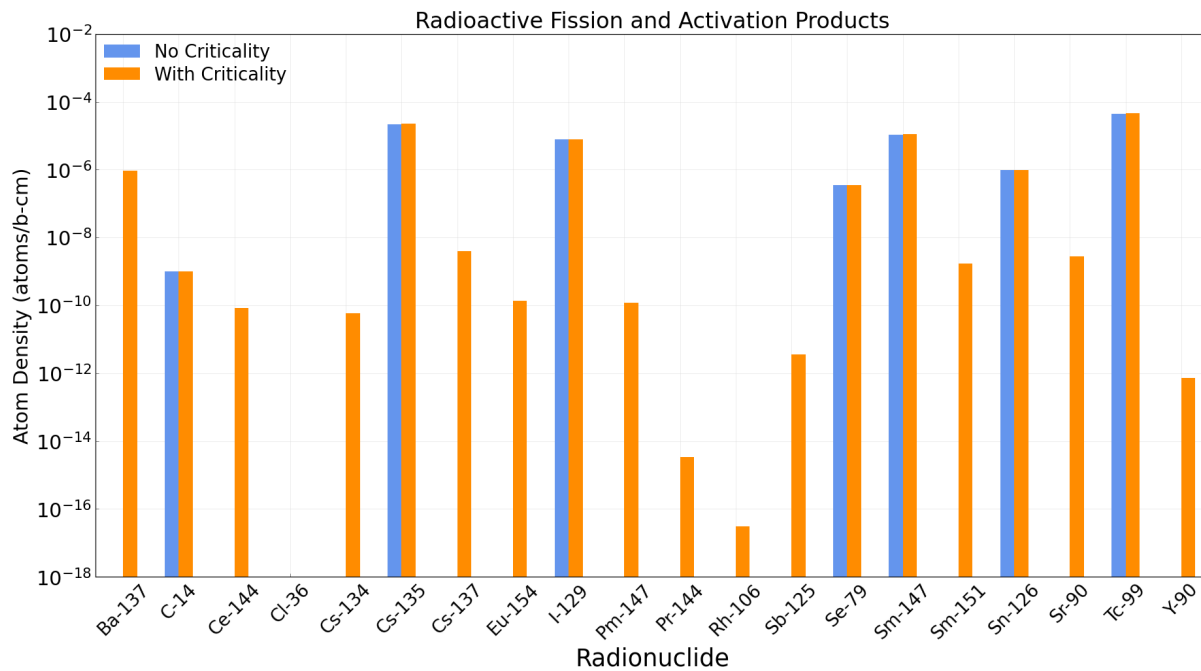


Figure 4. Comparison of radioactive fission product densities in the MPC-32-162 model with and without a 10,000 year criticality event producing 2.47 kW.

3. EVALUATING TH TOOLS FOR BOILING CANISTERS

3.1 MOTIVATION

A key objective of the thermal-hydraulic analysis is to accurately calculate fuel temperatures and moderator densities for feedback to the neutronic calculation. Calculating these quantities is especially difficult under two-phase fluid conditions, requiring accurate representation of the following physical phenomena:

1. liquid-vapor interface (water level) elevation,
2. subcooled liquid boiling,
3. vapor superheating,
4. two-phase boiling heat transfer between the solid structures (fuel rods, basket walls, canister walls) and the coolant, and
5. impact of local coolant density / void fraction on local fuel rod heat generation rate.

Liquid water is far denser than vapor (1,600 times denser at atmospheric pressure, and 30 times denser at 5 MPa, which is the hydrostatic pressure imposed on a DPC buried 500 m in a saturated repository). The liquid phase is also far more effective at removing heat from the fuel rods than the vapor phase, which impacts fuel temperatures. These create moderator reactivity feedback, which impacts not only the spatial heat generation distribution, but also overall canister criticality. This is why accurate calculation of not only the overall boiling rate but also the liquid and vapor spatial distributions throughout the canister are of high importance.

268 Therefore, a primary objective of this FY's modeling efforts was to determine RELAP5-3D's suitability
269 for predicting the two-phase phenomena listed above. In FY22, RELAP5-3D was found to provide reason-
270 able predictions under single-phase liquid conditions within the canister compared with computational fluid
271 dynamics (CFD). However, after assessing RELAP5-3D's capabilities and performance under two-phase
272 conditions in the current FY, it was found that RELAP5-3D does not provide the necessary modeling ca-
273 pabilities for predicting the water level's spatial location and its impact on canister performance given the
274 particular geometric configuration of this system. A review of the capabilities of a variety of TH codes
275 determined that the US Nuclear Regulatory Commission's TRACE code provides modeling features more
276 suitable for resolving these phenomena in DPC. In particular, TRACE allows three dimensional modeling of
277 the DPC fluid regions in a cartesian geometric representation, whereas RELAP5-3D only allows cylindrical
278 modeling in three dimensions. The cartesian representation allows realistic modeling of the liquid level and
279 gravitational effects for this horizontal canister configuration. It also aligns conveniently with the grid-like
280 arrangement of the basket assemblies in the canister, allowing explicit modeling of the flow within each
281 basket separately. This is intended to be done in the final TRACE model, whereas the cylindrical vessel
282 does not allow representing the grid-like assembly layout in this way. An additional benefit of TRACE
283 over RELAP5-3D is its ability to model fluid heat conduction, which allows fluid-to-fluid heat transfer even
284 under low flow conditions such as are expected in the DPC. A detailed discussion and supporting results are
285 presented in the remainder of this section.

286 **3.2 FY22 FULL-SCALE DUAL-PURPOSE CANISTER MODEL**

287 In Swinney et al. [3], the liquid temperatures (liquid subcooling) over time inside a horizontal $1/4$ -scale
288 DPC canister were calculated using both RELAP5-3D and the STAR-CCM+ code. This comparison showed
289 relatively good agreement, indicating that heat transfer was modeled reasonably well in RELAP5-3D under
290 single-phase conditions. However, additional investigation suggested that it was necessary to more closely
291 evaluate the applicability of RELAP5-3D in simulating this model when extending to two-phase flow.

292 The outer wall of the DPC is essentially cylindrical in shape and oriented in a horizontal direction. It
293 contains 32 basket assemblies of fuel rods, which are also oriented horizontally. A lateral cross section
294 of the arrangement of basket assemblies within the DPC is shown in Table 1. Figure 5 shows how these
295 32 basket assemblies were grouped in the FY22 RELAP5-3D model, and Figure 6 shows the component
296 layout of the entire RELAP5-3D model. The 32 basket assemblies were grouped into three concentric rings
297 based on their proximity to the radial center of the DPC. A fourth fluid region was modeled representing the
298 flow region between the outermost basket walls and the DPC cylindrical wall. This grouping of assemblies
299 and flow regions was a logical choice in terms of representing the radial convection and conduction of heat
300 from the more central assemblies of the DPC outward toward the outer assemblies and outer structures of
301 the DPC. This grouping scheme allowed the highest temperature to be predicted in the central assemblies
302 and decreasing temperatures towards the outer radius of the canister, which is the expected impact of radial
303 conduction and convection.

304 However, the FY22 model had a significant shortcoming because it did not realistically represent a
305 vertical flow distribution within each flow region; nor did it represent the resulting impact of the flow and
306 heat transfer caused by bulk natural circulation throughout the canister. In the RELAP5-3D component
307 layout shown in Figure 6, the four flow channels ("Outer 16," "Middle 12," "Central 4," and "Canister")
308 are all modeled as having a single vertical position and connected at common plena on the left and right.
309 Natural circulation is driven by differences in fluid densities at different vertical positions; therefore, the lack
310 of axial dependence in the FY22 RELAP5-3D model prevents natural circulation to be predicted throughout
311 the canister.

312 Natural circulation/convection is a potentially significant heat transfer contributor that impacts the pre-
313 dicted canister thermal behavior. The FY22 RELAP5-3D and STAR-CCM+ results showed reasonable

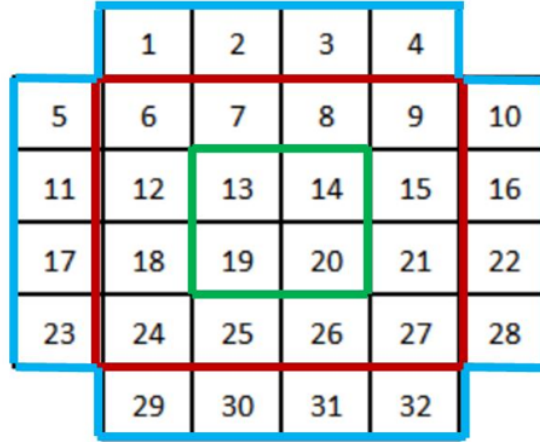


Figure 5. Side-view of the three-ring setup used in the FY22 RELAP5-3D MPC model.

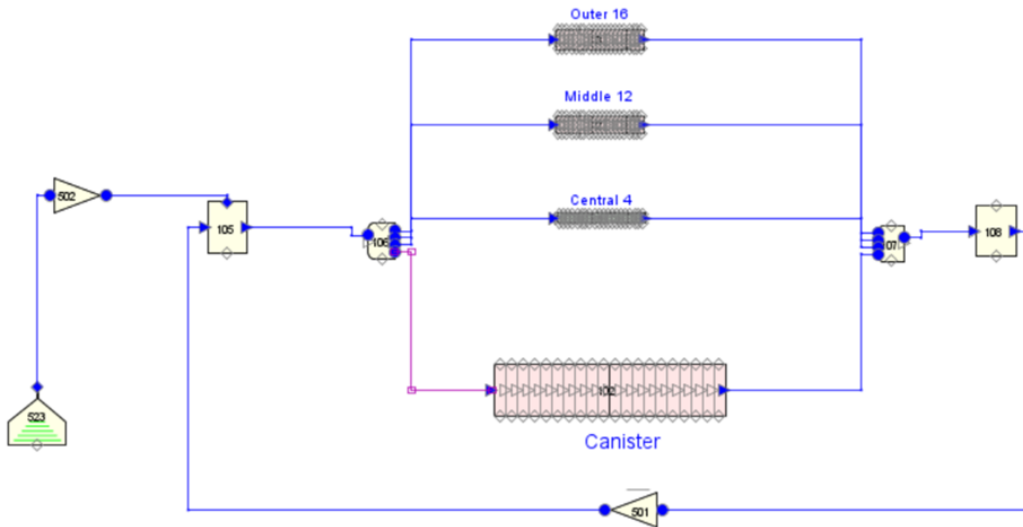


Figure 6. Component diagram for the FY22 RELAP5-3D MPC model.

314 agreement between the codes for single phase conditions; however, as discussed in the previous section,
 315 two-phase conditions introduce significant additional modeling challenges which can lead to far larger dis-
 316 crepancies in results than would be seen under single-phase conditions. Importantly, the FY22 RELAP5-3D
 317 model provides no means of predicting the vertical gas/water interface level within the canister and there-
 318 fore does not account for the potentially large vertical gradients in temperature and fluid conditions resulting
 319 from a two-phase mixture.

320 3.3 FULL-SCALE DUAL-PURPOSE CANISTER VERTICAL PIPE MODEL

321 The three-ring core treatment in the FY22 RELAP5-3D model was replaced with a vertical pipe con-
 322 figuration to realistically model the vertical differences among the assemblies. Although the canister con-
 323 figuration is horizontal, it was modeled in RELAP5-3D using a vertical pipe component. The vertical pipe
 324 was made up of 8 cells. The rows of assemblies (i.e., assemblies 1–4, 5–10, 11–16, etc., shown in Figure 7)
 325 were grouped as separate heat structures and were connected to a separate cells of the pipe, with the two
 326 remaining cells representing the canister volume above and below the assembly basket. The setup of the
 327 vertical pipe representing the canister is detailed in Figure 7), and the heat structure grouping is detailed in
 328 Figure 8.

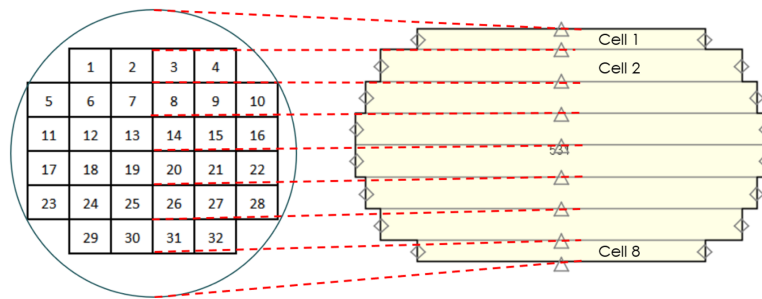


Figure 7. Vertical pipe setup used in RELAP5-3D DPC model.

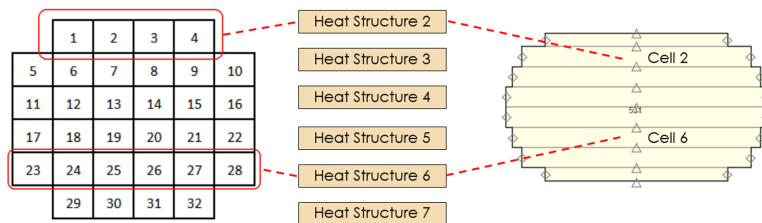


Figure 8. Heat structure grouping scheme used in RELAP5-3D MPC model.

329 Under two-phase conditions, the vertical pipe modeling scheme allows RELAP5-3D to calculate the
 330 water level either at the boundaries between vertical cells or in some fraction of the way along a cell. This
 331 provides a realistic vertical distribution of void fraction and mixture water density that allows RELAP5-3D
 332 to accurately determine the local wall-to-fluid heat transfer coefficient, buoyancy terms, frictional terms, and
 333 other parameters for the fluid solution. It also allows RELAP5-3D to provide realistic vertically dependent
 334 local fluid mixture densities to the neutronics calculation.

335 Another advantage of modeling the horizontal canister using a vertical pipe was the ability to connect
 336 the void fraction of the canister to the power level of each assembly row. For example, in reality, the top
 337 row of assemblies (cells 1–4 in Figure 8) will produce full power when the pipe cell connected to this row
 338 is full of water and will produce zero power when the water in this cell has boiled off. Although the model

339 and power tables in RELAP5-3D were set up to follow this behavior, the power level in all assemblies was
 340 ultimately kept constant to more closely match the setup used in STAR-CCM+.

341 A primary drawback of the vertical pipe approach is that it neglects temperature and fluid variations in
 342 the axial direction (i.e., horizontal direction along the length of the fuel rods). The FY22 model did account
 343 for axial variation, which is an important effect in the DPC because of the axial power distribution, which is
 344 highly skewed toward one end of the fuel. An approach for modeling axial and vertical variation simultane-
 345 ously is discussed below. However, the vertical pipe approach is presented here as the best available option
 346 in RELAP5-3D, at least in terms of modeling two-phase conditions.

347 A small hole on the side (which is the top in this horizontal configuration) of the canister was modeled
 348 in RELAP5-3D using a check valve. This valve was intended to allow steam to exit the system while
 349 preventing liquid water from entering the system. The model boundary was assumed to be adiabatic with no
 350 heat being exchanged with the environment outside the canister wall. This was accomplished in RELAP5-
 351 3D by modeling the canister as a pipe without any connection to any heat structures that would represent
 the canister wall or surrounding rock. A diagram of the RELAP5-3D model is provided in Figure 9.

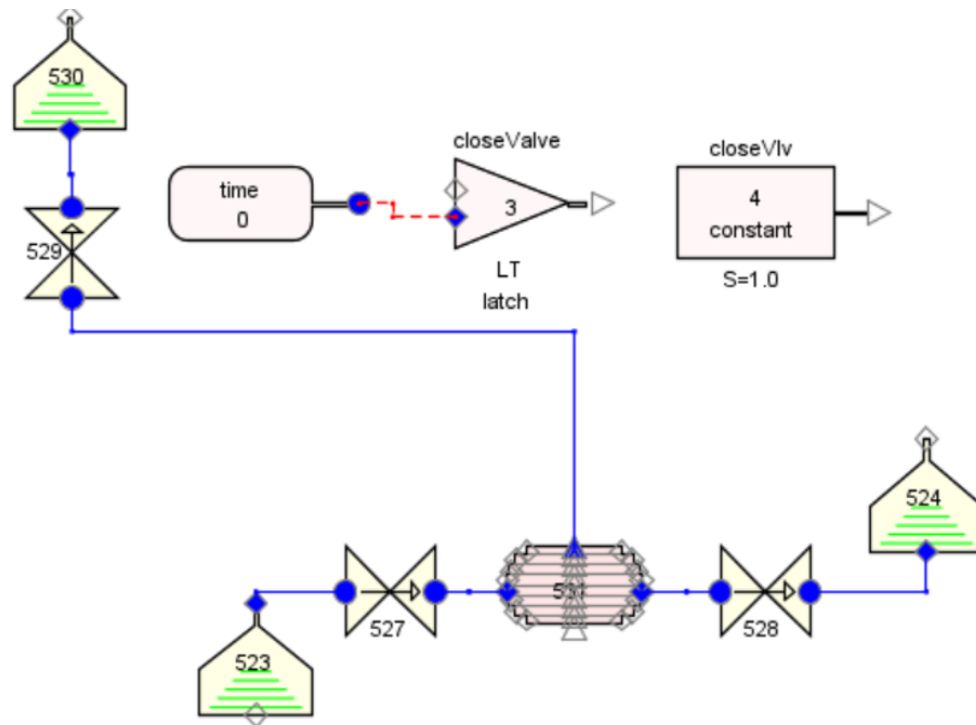


Figure 9. Full-scale DPC RELAP5-3D model.

352

353 Relevant dimensions and initial conditions for the full-scale DPC are provided in Table 3.

354 3.3.1 STARCCM+ SIMULATION

355 In this subsection, the setup used for simulating boiling in a representative canister using STAR-CCM+
 356 is discussed.

357 Geometry

358 In FY 2022, a quarter portion of the MPC32 canister, as shown in Figure 10 (left) was used for CFD
 359 modeling and comparison with RELAP5-3D, under the assumption of flow symmetry, to save excessive

Table 3. Dimensions and initial conditions for an MPC-32 boiling case.

Parameter	Value
Canister volume (m ³)	7.96
Initial liquid volume (m ³)	7.20
Initial liquid volume fraction (%)	90.5
Pressure (Pa)	4.5×10 ⁶
Initial fluid / gas temperature (K)	530.59
Canister power (kW)	100
Simulation time (s)	365

360 computational cost. However, such an assumption is valid only for vertically placed fully flooded canisters
 361 in a repository. The original placement of the canister is nearly horizontal, with its major axis nearly parallel
 362 to the ground, so the flow is not expected to be strictly repeatable for each quarter of the canister. Therefore,
 363 the previous geometry was replaced with the geometry shown in Figure 10 (right). The symmetries of flow
 364 are still leveraged to save computational cost, but vertical planes of symmetry are assumed in this study
 365 with normal orientation parallel and perpendicular to the major axis. The final geometry seen in Figure 10
 366 (right) was selected for this study based on the best trade-off between physically realizable representation of
 canister placed in a repository and CFD calculation expense.



Figure 10. Geometries considered for CFD modeling: previous (left) and current (right).

367

368 Mesh

369 Polyhedral mesh elements were used to discretize the geometry (see Figure 11) because of their ability
 370 to easily resolve the complex spacings (inter-rods, basket-to-rod, etc.) and to conform to the complex
 371 curvilinear boundaries of the canister geometry with a smaller mesh count. They are also known to have
 372 faster solution convergence than hexahedral mesh elements. Two cells were inserted between the rods to
 373 capture the boiling bubble evolution; however, two cells may not be sufficient to accurately resolve inter-rod
 374 thermal hydraulics. Even with just two cells, the total mesh count for the canister geometry approached 126
 375 million cells; hence, insertion of more cells in the inter-rod spacings was not attempted. It was decided to
 376 proceed with this mesh for the simulation.

377 Setup and postprocessing

378 A total of 256 cores on the Ridge compute cluster operated and maintained by the Compute and Data
 379 Environment for Science (CADES) at ORNL was used to conduct the boiling simulations. Because of the
 380 excessive computational cost involved in conducting a transient simulation of such a large system, a variable
 381 time-step was adopted. Initially a very low time-step of 10⁻⁴ was used and was progressively increased to
 382 0.01 s. Despite this strategy, the simulation runtime still remained approximately 5 days, and a data file
 383 of 140 GB was generated in the process. The liquid mass loss caused by boiling over time was chosen as

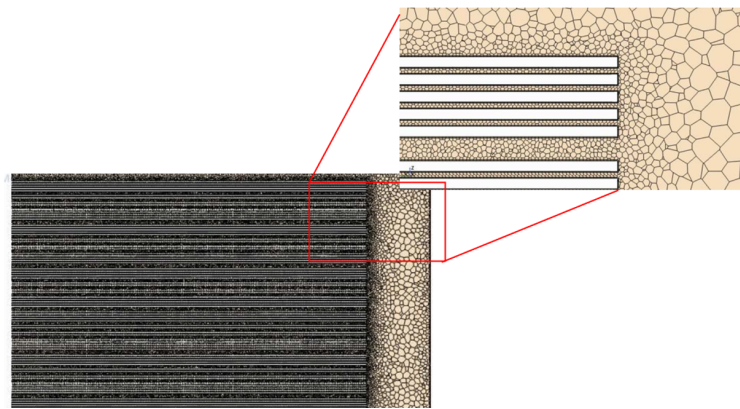


Figure 11. Mesh on a plane cutting the fuel rods.

384 the parameter of interest in this comparison. Because the liquid level over time is not easily calculated in
 385 RELAP5-3D, the liquid mass loss was intended to serve as an analog to the liquid level over time. Ultimately,
 386 the change in the liquid level, which can be calculated from the liquid mass loss, will be the input to the
 387 neutronics calculations

388 3.3.2 RESULTS

389 The liquid volume fraction, fluid temperature, and vapor temperature in each pipe cell were calculated
 using RELAP5-3D at 365 s and are provided in Table 4.

Table 4. Predicted fluid properties for fullScale MPC-32

Cell	Liquid volume fraction (%)	Fluid temperature (K)	Vapor temperature (K)
1	0	530.56	531.05
2	0.67	530.69	531.22
3	0.99	530.66	530.59
4	0.99	530.69	530.61
5	0.99	530.73	530.64
6	0.99	530.78	530.66
7	0.99	530.81	530.69
8	1	530.59	530.71

390

391 The liquid mass loss predicted by each code was compared at an arbitrary simulation time. An analytic
 392 calculation was also performed as a point of comparison. The analytic calculation assumed saturated liquid
 393 and vapor conditions, with the 100 kW power being translated into a boiling rate based on the heat of
 394 vaporization of water at 4.5 MPa. This heat of vaporization was taken from NIST thermophysical property
 395 data for water, which is expected to produce close agreement to the TRACE and RELAP5-3D built-in
 396 thermophysical property data.

397 The liquid mass loss predicted by each code and by the analytic calculation are provided in Table 5.
 398 The liquid mass loss calculated by RELAP5-3D generally matched the analytic solution but was approxi-
 399 mately 4 times smaller than the value predicted by STAR-CCM+. The overprediction of liquid mass loss
 400 by StarCCM+ compared to analytic solution and RELAP is still under investigation. The excessive com-
 401 putational cost involved in performing these simulations prohibited the multiple simulation trials necessary

402 to effectively troubleshoot the problem. Therefore, the goals for the efforts in the subsequent sections were
 403 to conduct verification studies on simplified small-scale geometries to conveniently isolate the root cause of
 404 the problem, seek a quick solution to it, and compare predictions for both codes effectively. Then, a return
 to the real-scale canister model could be performed during the final phases of the verification plan.

Table 5. Predicted liquid mass loss comparison for full-scale MPC-32

	RELAP5-3D	Star-CCM+	Analytic
Power(kW)	100	100 (25×4)	100
Initial liquid mass (kg)	5,672.53	5,673 (1,418×4)	5,672.53
Final liquid mass (kg)	5,648.92	5,536 (1,384×4)	5,650.75
Liquid mass loss (kg)	23.61	137	21.78

405

406 3.4 SIMPLE BOILING TEST CASE

407 Because of the lack of agreement in the liquid mass loss between the full-scale DPC as modeled in
 408 RELAP5-3D and STAR-CCM+, a simple test case involving boiling water was devised. This simplified
 409 boiling test case was intended to remove the complexities associated with modeling boiling in both codes.
 410 For this case, a vertical cylinder of water was modeled using a single-cell in RELAP5-3D. The cylinder
 411 of water was heated by a heating element, and the liquid volume mass lost from boiling over time was
 412 monitored.

413 The RELAP5-3D model consisted of three main components: a single-celled pipe representing the
 414 cylinder, a valve representing the open face of the cylinder, and a time-dependent volume representing the
 415 surrounding environment. Heat was supplied to the cylinder through a powered heat structure. A diagram
 of the RELAP5-3D model is provided in Figure 12.

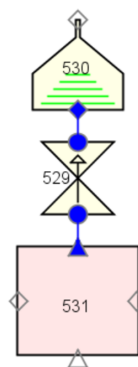


Figure 12. Simple boiling test case RELAP5-3D model.

416

417 Relevant dimensions and initial conditions for each case are provided in Table 6.

418 3.4.1 STARCCM+ SIMULATION SETUP

419 The boiling model, meshing strategy, and quantity compared for both codes were retained from Sec-
 420 tion 3.3 for this comparison study. The geometry considered for the STAR-CCM+ study is provided in
 421 Figure 13. The dimensions of the geometry and the initial conditions used for simulation are given in
 422 Table 6. Figure 14 shows the evolution of bubbles generated on the rod's surface moving in the upward

Table 6. Dimensions and initial conditions for simple boiling case

Parameter	Value
Volume (m³)	0.021
Initial liquid volume (m³)	0.014
Initial liquid volume fraction (%)	65.4
Rod height (m)	0.18
Rod radius (m)	0.2
Pressure (Pa)	4.5e6
Initial fluid / gas temperature (K)	530.59



Figure 13. Simple boiling test case RELAP5-3D model.

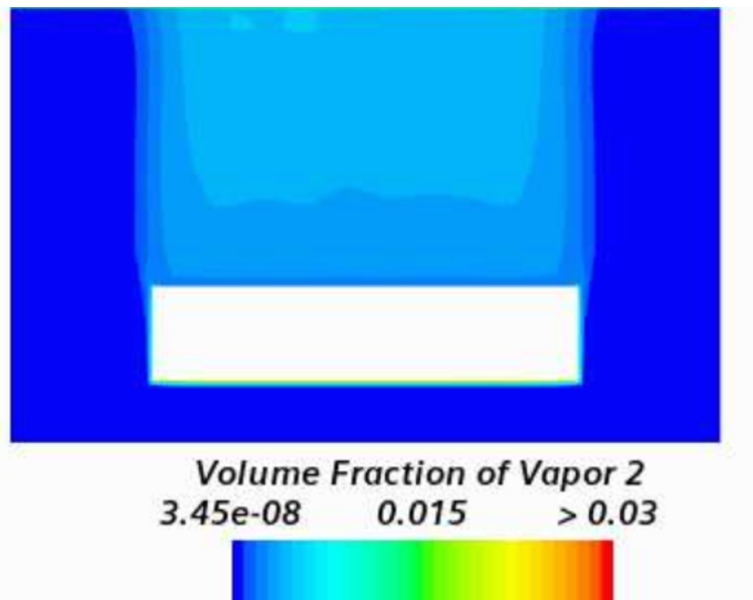


Figure 14. Volume fraction of bubbles on a cut-section of the geometry.

423 direction as a result of buoyancy through the water phase. The amount of vapor generated is tracked and
 424 deducted from the liquid mass to calculate the liquid mass loss required for comparison.

425 The liquid mass loss predicted by each code was compared at an arbitrary simulation time. An analytic
 426 calculation was also performed as a point of comparison. The liquid mass loss predicted by each code
 427 and by the analytic calculation are provided in Table 7. The liquid mass loss predicted by RELAP5-3D
 428 matched the analytic calculation, whereas the liquid mass loss predicted by STAR-CCM+ was higher than
 429 the analytic calculation in both cases, as observed in Section 3.3.2. The overprediction could be caused by
 430 the larger timestep adopted or the variation of heat of vaporization with pressure, which is held constant
 431 for StarCCM+ simulation. These possible causes for overprediction will be explored and resolved in future
 432 work. Field functions will be generated to account for the variation of heat of vaporization with pressure
 433 and will be used to conduct high-fidelity simulations of more complex test problems for boiling to verify the
 systems code (RELAP5-3D or TRACE) for cases in which analytical solutions are not feasible.

Table 7. Predicted liquid mass loss comparison for simple boiling cases

	Case 2 (submerged rod)		
	RELAP5-3D	STAR-CCM+	Analytic
Power (W)	904		
Simulation time (s)	386		
Initial liquid mass (kg)	10.92	10.92	10.92
Final liquid mass (kg)	10.72	10.63	10.73
Liquid mass loss (kg)	0.20	0.285	0.19

434

435 3.5 2D CANISTER MODELING WITH TRACE

436 Because of ongoing uncertainty about the applicability of RELAP5-3D for simulating critical DPCs,
 437 TRACE was chosen to be investigated as a thermal analysis code capable of modeling a horizontal DPC

438 with liquid loss caused by boiling. The “3D vessel” component in TRACE is capable of discretization using
439 a Cartesian coordinate system and is capable of blocking flow between selected adjacent cells. Therefore,
440 TRACE is better suited to capture the physics of a horizontal system with channel walls preventing flow
441 in the vertical direction. This capability allows accurate representation of both the vertical direction (i.e.,
442 accurate representation of the two-phase water level and local two-phase effects) and the axial direction (i.e.,
443 accurate representation of the axially dependent power profile) in the DPC canister simultaneously.

444 Note that RELAP5-3D has a 3D vessel capability, but it is restricted to cylindrical (r, z, θ) geometry. For
445 the DPC, the z coordinate would be along the horizontal axial length of the fuel assemblies, and the polar
446 (r, θ) coordinates would be a lateral circular cross section of the canister. For the case of a horizontal cask
447 such as a DPC, the polar geometry makes it impossible to accurately track the two-phase water level because
448 the radial and azimuthal sectors do not align with a given horizontal plane (i.e., they cannot accurately
449 resolve the water level elevation). The Cartesian vessel in TRACE can resolve this elevation accurately,
450 whether the water level elevation is at the boundary between two vertical cells or at some fraction of elevation
451 within a given cell.

452 Also, since the assemblies are arranged in a grid-like pattern in the canister, the cartesian vessel will
453 allow modeling the flow in each assembly explicitly, which is the ultimate goal of the TH analysis. RELAP5-
454 3D, which allows only cylindrical modeling in three dimensions, is not suited to accomplish this.

455 An additional benefit of TRACE over RELAP5-3D is its ability to model fluid heat conduction, which
456 is likely significant for the low flow rate conditions expected in the DPC. This would allow TRACE to
457 predict heat transfer between fluid cells in a reasonable manner even under very low flow or stagnant flow
458 conditions, whereas RELAP5-3D would not be able to predict the fluid-to-fluid heat transfer in this situation.

459 3.5.1 2D TEST PROBLEM

460 A simplified test problem similar to that required for a horizontal DPC was devised to investigate the
461 potential applicability of TRACE. Initially, the test problem consisted of a simple rectangular prism full of
462 water with a single submerged heat source (similar to the simplified boiling case 2 modeled in RELAP5-3D).
463 For various reasons, the following features were also added to the model:

- 464 • Steel channel walls were added around the rod, creating a central fluid channel. These channel walls
465 were added to prevent flow between specific cells in the vertical direction.
- 466 • Steel walls were added to the faces of the vessel in both the vertical and horizontal directions. A
467 300 K boundary temperature was established on these walls. The other two vessel faces were kept as
468 adiabatic. These walls were added to improve the heat removal rate from the fluid vessel; furthermore,
469 the heat removed through each wall could be compared between each code.
- 470 • Two pressurizers that were modeled as vertical pipes filled with vapor at the same pressure as the
471 main vessel were placed above the vessel and connected to the uppermost face. The purpose of these
472 pressurizers was to prevent any large pressure increase in the vessel fluid.
- 473 • An axial power profile was applied to the heated rod to intentionally create a flow pattern and a fluid
474 temperature distribution that would theoretically be similar in both codes. Before switching to the
475 axial power profile, TRACE showed a “hysteresis” effect in which the fluid would arbitrarily start
476 flowing in one direction, even though the power profile was initially entirely symmetric. The axial
477 power profile used for this test problem was adapted from an 18-cell power profile used in DPC
478 neutronics calculations [2].

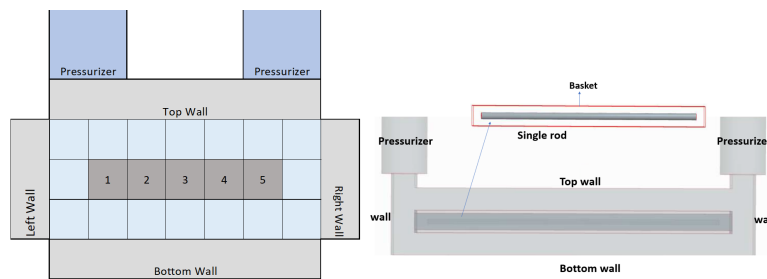


Figure 15. Representation of test problem (not to scale): TRACE (left) and CFD (right).

479 A visual representation of this test problem for TRACE and StarCCM+ is provided in Figure 15; this
480 figure shows the four walls through which heat losses were compared and indicates the five fluid cells in
481 which temperature changes were compared.

482 The test problem as modeled in TRACE is shown in Figure 16. The TRACE model consisted of a vessel
483 component connected by single junctions to two pipes representing the pressurizers. A cylindrical heat
484 structure was used to model the heated rod. Planar heat structures were used to model the walls surrounding
the central channel and the walls surrounding the main vessel.

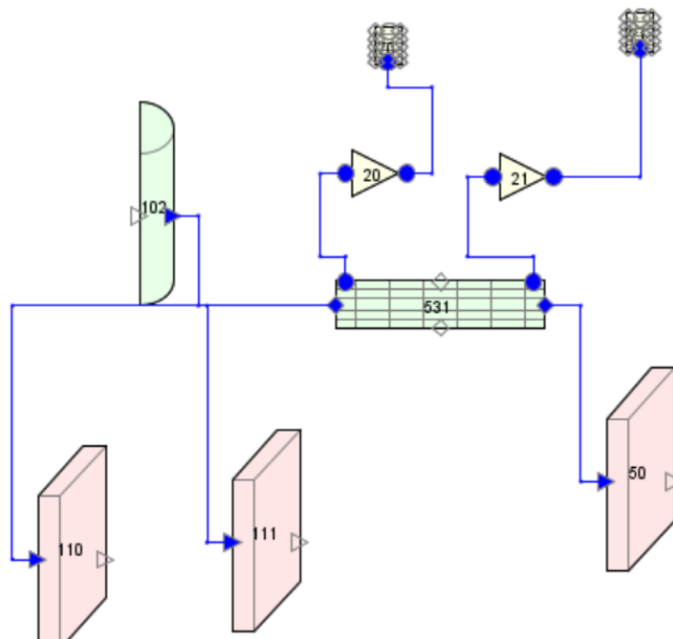


Figure 16. Test problem TRACE model.

485

486 Relevant dimensions and initial conditions for the TRACE test problem are provided in Table 8. The
487 axial power profile is provided in Table 9.

488 Once base case results were obtained, the TRACE grid mesh was further refined by increasing the
489 number of cells in the vessel. Cells were added to various specific areas of the vessel to investigate the
490 impact of the refined mesh on heat loss through each wall, as well as the fluid temperature in the central
491 channel. A total of eight cell refinement schemes were compared; each refinement scheme is shown in
492 Figure 17. The 10-axial cases refer to 10 axial cells along the length of the fuel (with an additional left- and
493 right-hand node at the ends of the canister), compared to 5 axial fuel cells in the base case. For any case in

Table 8. Dimensions and initial conditions for TRACE test problem

Parameter	Value
Vessel volume (m ³)	3.24×10^{-3}
Pressurizer volume (m ³)	5.0×10^{-4}
Channel and outer wall thickness (m)	0.01
Pressure (Pa)	1.01325×10^5
Initial fluid temperature (K)	300.0
Initial vapor temperature (K)	530.587
Total power (W)	500
Simulation time (s)	2×10^4

Table 9. Axial power profile used in TRACE test problem

Fluid cell	Power fraction (%)	Cell power (W)
1	89.435	447.175
2	10.089	50.443
3	0.450	2.250
4	0.025	0.124
5	0.001	0.007

494 which the central row of cells was divided in the vertical direction, the heat structure representing the heated
 495 rod in TRACE was divided to match the vessel cells because TRACE is unable to connect heat structures to
 496 more than one fluid cell simultaneously.

497 3.5.2 STAR-CCM+ SIMULATION

498 The geometry used for the STAR-CCM+ simulation is given in Figure 15. A two-phase volume of fluid
 499 method with a Reynolds-averaged Navier Stokes (RANS) simulation model was used to predict the natural
 500 circulation and associated heat transfer inside the system. The initial liquid level in the bottom of the tank
 501 was initialized using a field function for the volume fraction of the liquid. The variation of water density with
 502 respect to the temperature was accounted for using steam tables from The International Association for the
 503 Properties of Water and Steam [18]. An asymmetric power profile as given in Table 9 was applied to the rod.
 504 The simulation was run until the net accumulation of heat reached zero and the total power produced by the
 505 rods was balanced by the total power dissipated through the walls of the system. The temperatures predicted
 506 at steady-state were volume averaged on five boxes arranged axially along the rod for comparison with
 507 TRACE. Figure 18 shows the temperature map inside the system. The highest temperatures are observed at
 508 the left end as a result of the peaking of the power. Local temperatures on the surface of the rod on the left
 509 end reached the boiling point because of the high concentration of power in that region. Figure 19 shows the
 510 natural circulation pattern predicted by the simulation. Natural circulation is dominant in the upper section,
 511 so the heat transfer rate through the upper wall is the highest there compared to the other walls as reported
 512 in the heat transfer budget presented in Table 11.

513 3.5.3 2D TEST PROBLEM RESULTS

514 Cell-averaged fluid temperatures in the five central cells were calculated using both TRACE and STAR-
 515 CCM+ and are provided in Table 10. The heat losses through each of the four walls surrounding the main
 516 vessel were calculated using both codes and are provided in Table 11. The fluid temperatures in the base case
 517 showed a profile generally similar to that predicted by STAR-CCM+ but with lower temperatures throughout

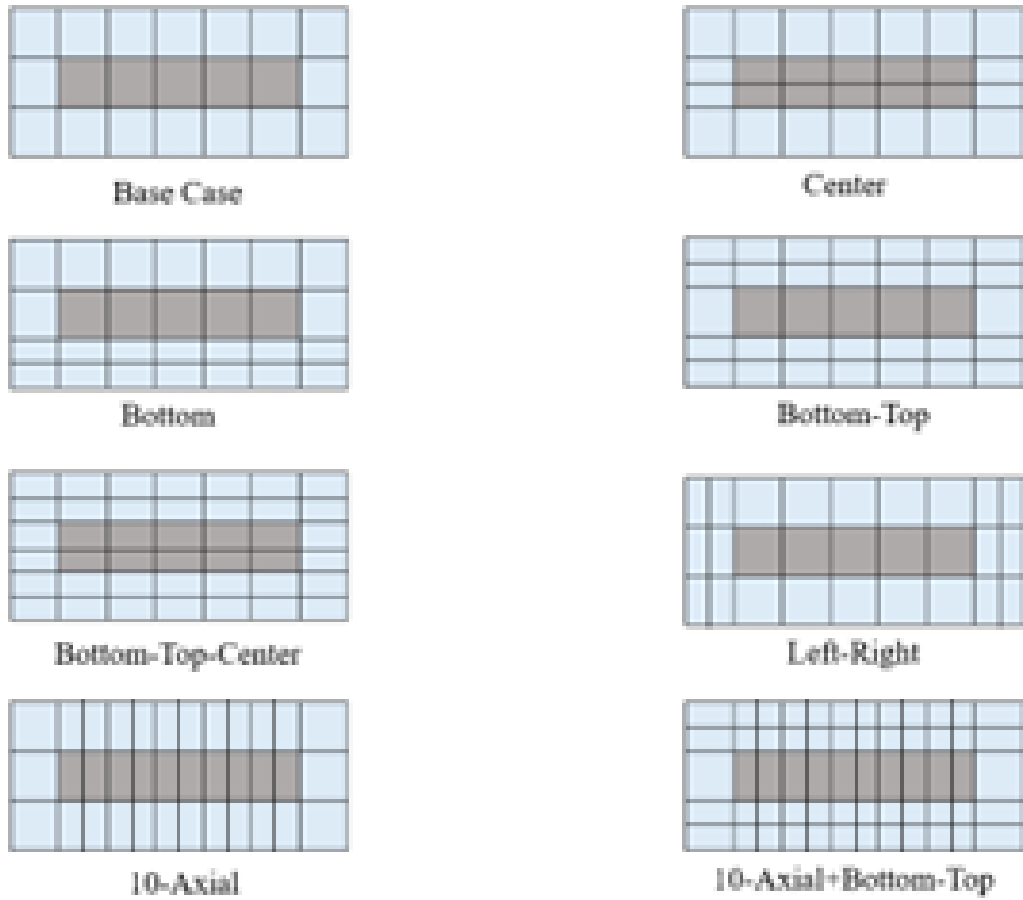


Figure 17. Vessel cell refinement schemes used in TRACE test problem.

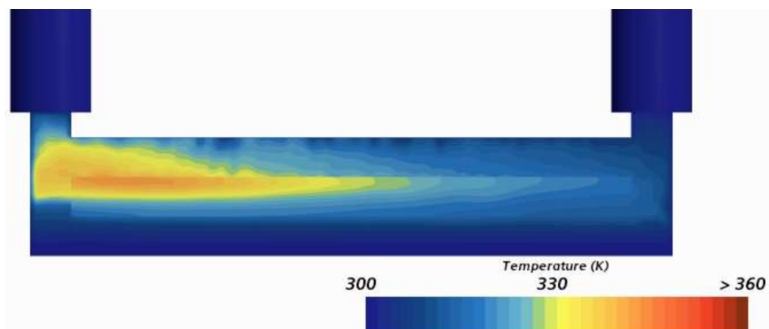


Figure 18. Temperature contour predicted by CFD on a cut section.

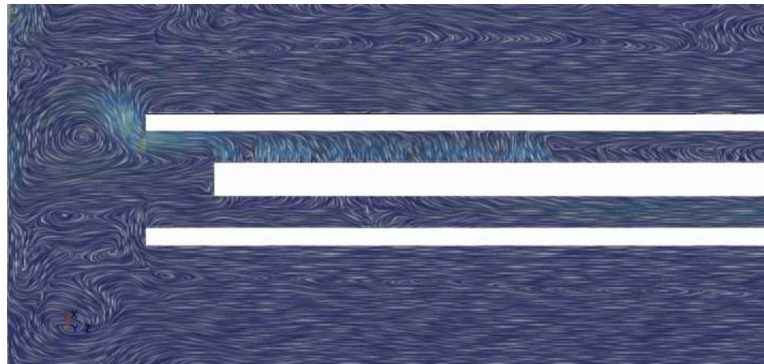


Figure 19. Natural circulation contour predicted by STAR-CCM+ on a cut section.

518 and a greater temperature descent from cells 1 to 2. This implies that too much heat was being removed from
519 cell 1 because of the relatively coarse cell mesh in the horizontal direction. The results also indicate that
520 the base case TRACE model rejected too much heat through the bottom wall because of the relatively small
521 number of fluid cells in this region; adding cells near the bottom of the vessel resulted in fluid temperatures
522 and wall heat losses that more closely matched the values predicted by STAR-CCM+.

523 As shown in these results, both the vertical and horizontal discretization in TRACE significantly im-
524 pacted the temperature and heat loss distributions. In addition to simply increasing the spatial fidelity, the
525 inclusion of additional nodes allows more complex flow patterns and more detailed spatial effects to be
526 represented in the TRACE model. For example, STAR-CCM+ predicted counter-current flow in the upper
527 region of the canister, with flow moving left to right along the upper canister wall and right to left along
528 the top of the upper basket wall (Figure 18). A TRACE model with only a single row of cells in this up-
529 per region would not be able to model this bi-directional behavior due to the excessive coarseness of the
530 mesh. Having two or more rows of cells in this region does permit this possibility. A similar argument
531 can be made for the fuel assembly region as well as the left and right plenum regions, which are additional
532 locations where STAR-CCM+ predicts counter-current flow. Further analysis is necessary to assess whether
533 TRACE is predicting such counter-current behavior in the refined models. Another possible impact is fluid
534 heat conduction, which is modeled in TRACE and allows heat transfer even under low-flow conditions; this
535 phenomenon is better resolved for finer meshes. Note that, unlike STAR-CCM+, TRACE does not include
536 all of the momentum and energy transport terms in the multidimensional fluid equations that are necessary
537 to finely resolve detailed phenomena such as eddies and vortices. Therefore, the TRACE solution is not nec-
538 essarily expected to precisely approach the STAR-CCM+ solution as further mesh refinements are made.
539 However, additional investigation will be performed to determine the optimal mesh for this scenario and
540 ensure the best agreement with STAR-CCM+. Once the optimal mesh is established for this simplified test
541 problem, a similar spatial fidelity will then be applied to a full scale canister model in TRACE to arrive at
542 best-estimate full canister predictions.

543 **3.6 PLANNED VERIFICATION WORK**

544 Significant additional work is required to verify whether TRACE is an acceptable tool for TH calcu-
545 lations in simulating boiling in a critical DPC. The following subsections briefly describe the verification
546 work planned for next year.

547 **3.6.1 SINGLE-PHASE WATER FLOW**

548 Additional simulations to investigate TRACE's water flow predictions are necessary to ensure that the
549 natural circulation calculations in TRACE are accurate. Future verification problems include the following:

Table 10. Cell temperatures in the TRACE cases and the Star-CCM+ case for the 2D problem

	Cell-average fluid temperature (K)				
	1	2	3	4	5
Base case	321.85	313.42	312.51	312.52	312.58
Center	314.84	315.14	315.12	315.08	315.05
Bottom	324.05	314.97	313.88	313.81	313.79
Bottom-top	324.25	315.58	314.53	314.43	314.38
Bottom-top-center	315.06	313.81	313.87	313.57	313.52
Left-right	318.33	318.92	318.77	318.58	318.40
10-axial	319.62	321.70	321.44	321.08	320.73
10-axial+top-bottom	324.13	315.70	314.86	314.85	314.91
STAR-CCM+	330.93	327.53	323.08	319.50	316.94

Table 11. Wall heat loss in the TRACE cases and the Star-CCM+ case for the 2D problem

	Wall heat loss (W)				
	Top	Bottom	Left	Right	Total
Base case	301.88	91.36	59.39	46.17	498.79
Center	225.19	180.10	47.13	46.76	499.17
Bottom	338.19	39.42	68.32	52.77	498.70
Bottom-top	338.43	31.89	73.11	55.16	498.59
Bottom-top-center	356.62	20.41	70.29	51.39	498.72
Left-right	191.54	212.81	40.28	54.57	499.19
10-axial	293.94	103.21	44.26	57.36	498.77
10-axial+top-bottom	322.53	40.26	76.57	59.08	498.44
STAR-CCM+	350.77	1.92	112.4	31.5	496.59

550 1. Refined axial power profile

551 An axial power profile was included in the TRACE test problem developed for this report, but the
552 power profile only contained five cells. A power profile with 18 axial cells should be investigated to
553 match the axial segmentation used in the neutronics models.

554 2. Multiple channels in the Y and Z directions

555 Currently, only a single assembly channel was modeled. Modeling multiple channels in the z -direction
556 (along which gravity acts) with fluid plena on the left/right of the model will potentially demonstrate
557 the natural circulation loop where fluid exits some channels and enters others.

558 3. Multiple fuel rods inside one channel

559 Multiple rods inside one channel may be modeled in the z -direction to investigate the effect of the
560 physical placement of the rods on the overall liquid temperature.

561 4. Down-scaled canister

562 A down-scaled canister with multiple assemblies, plena on both ends, and an outlet on the side of the
563 canister, as shown in Figure 20, would combine the features of all previous cases and would represent
564 all the essential features of a full-scale DPC model on a reduced scale.

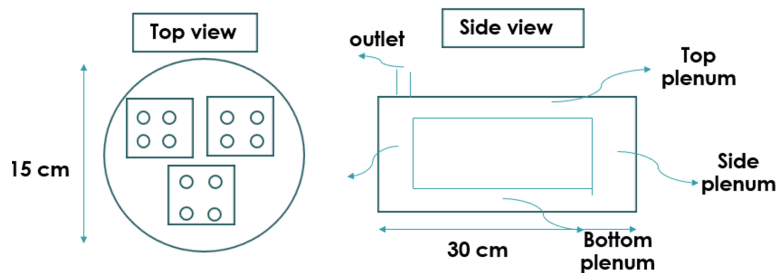


Figure 20. Down-scaled canister model.

565 **3.6.2 TWO-PHASE BOILING**

566 Once the natural circulation problems listed above have been verified, the two-phase boiling physics
567 must also be verified. The verification plan is to repeat the single-phase test cases presented above at a
568 power level sufficient to cause boiling. The goal of these simulations is to verify that TRACE is able to
569 accurately calculate the canister fluid level over time as the liquid boils. For the case with multiple fuel rods
570 inside one channel, although the full number of rods in the z -direction (i.e. 17) likely does not need to be
571 modeled, multiple cases may be necessary to determine the minimum number of modeled rods needed to
572 calculate the liquid loss with sufficient accuracy to be input to the neutronics model.

4. DPCS SEALED IN A BENTONITE BACKFILL

The scenario hypothesized in this section represents the least understood possibility of what could occur in the event of a DPC achieving criticality in a saturated geological repository. It involves a working theory that saturated bentonite clay could seal a DPC and prevent water or steam from escaping. Figure 21 depicts a cartoon version of a drift in which a canister is in a saturated clay backfill within a saturated rock formation. The basic assumptions for this scenario are as follows:

- Saturated bentonite has a very low permeability (10^{-18} to 10^{-20} m²).
- Water could infiltrate the canister slowly over centuries or millennia, but it would not be able to escape on the time-scale of a criticality event.
- Sufficient over-pressure may result in a fracture or “breakthrough,” allowing the escape of steam or water.
- This scenario could result in higher powers than can be achieved in a permeable backfill.

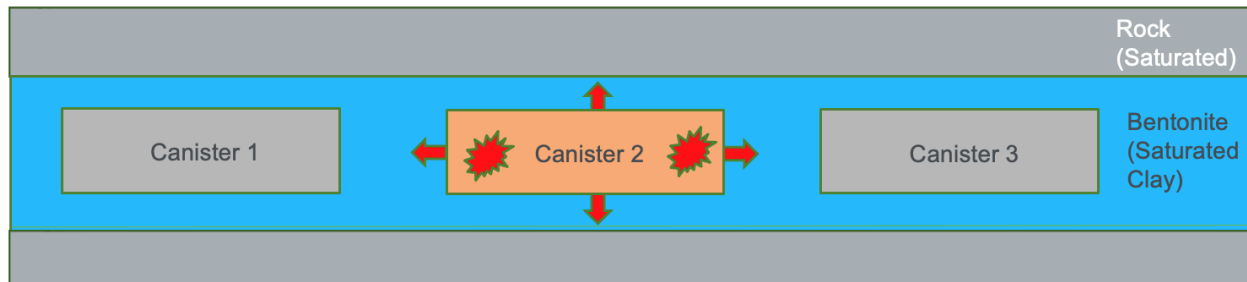


Figure 21. A depiction conceptualizing a DPC in a drift back-filled with bentonite.

This postulated circumstance is fundamentally different from previous scenarios because the moderator cannot expand to limit criticality. The primary feedback mechanism in this case will be Doppler broadening within the fuel itself. In previous scenarios, temperatures were relatively low, and this effect was negligible; however, in this scenario, the fuel temperature will increase rapidly until Doppler broadening provides sufficient negative feedback to achieve a k_{eff} near unity. Therefore, to model this scenario accurately, a radiation transport model with a temperature profile is necessary. However, the models generated with UNF-ST&DARDS have a homogeneous temperature throughout the model, and there is no existing mechanism for applying a varying temperature to the model.

To pursue analysis of this scenario, a new python-based parser tool was developed that reads a custom formatted temperature profile describing the fuel, clad, and water temperatures throughout the DPC and modifies the temperatures for the corresponding materials within a standard radiation transport model created with UNF-ST&DARDS. An example of the data used for an MPC-32 is shown in Table 12. The data are based on the simplified 3-ring RELAP5-3D model illustrated in Figure 5, so there are only three radial profiles. Once the higher fidelity TRACE-based TH model is developed, profiles for all 32 assemblies could theoretically be used to perform the analysis for this scenario in the future.

The initial workflow for analyzing the so-called “sealed” DPC began by providing the power distribution from the Shift model as input to RELAP5-3D. A power level is assumed, and RELAP5-3D generates the associated temperatures for the fuel and other components in the format shown in Table 12. The new parser script modifies the original UNF-ST&DARDS model to apply the new temperatures. Then, Shift is used to calculate the new multiplication factor of the system. This process is repeated until the Shift model

Table 12. Example temperature profile for sealed DPC (500 kW case)

Axial cell	201 Fuel center temp (K)	201 Clad outer temp (K)	Central fluid temp (K)
1	577.3	538.0	537.0
2	575.7	538.0	537.1
3	557.2	537.8	537.1
4	545.7	537.5	537.1
5	540.6	537.3	537.1
6	538.5	537.2	537.1
7	536.5	536.0	535.7
8	533.4	533.2	533.1
9	524.4	524.3	524.2
10	468.3	468.3	468.2
11	422.3	422.3	422.3
12	390.8	390.8	390.8
13	369.1	369.1	369.1
14	353.9	353.9	353.9
15	343.2	343.1	343.1
16	335.5	335.5	335.5
17	330.0	330.0	330.0
18	326.1	326.1	326.1

605 predicts a k_{eff} near unity, thus identifying the power level required to provide sufficient Doppler broaden-
 606 ing feedback within the fuel to limit criticality within the DPC. An example of this is shown in Figure 22.
 607 As shown in Figure 23, even at 5 MW, the pressure builds up rapidly within the canister. If these mod-
 608 els are accurate, then it would seem apparent that some sort of fracture or breakthrough would occur at
 609 these pressures, thus allowing for the water to boil. The ORNL research team is currently collaborating
 610 with the Geosciences Division at Lawrence Berkeley National Laboratory (LBNL) to perform geomechan-
 611 ics simulations to investigate this hypothesis. These calculations are being performed with the Transport Of
 612 Unsaturated Groundwater and Heat (TOUGH) code [19], which is designed for multi-phase fluid flow and
 613 heat transport in porous media coupled with a geomechanics simulator.

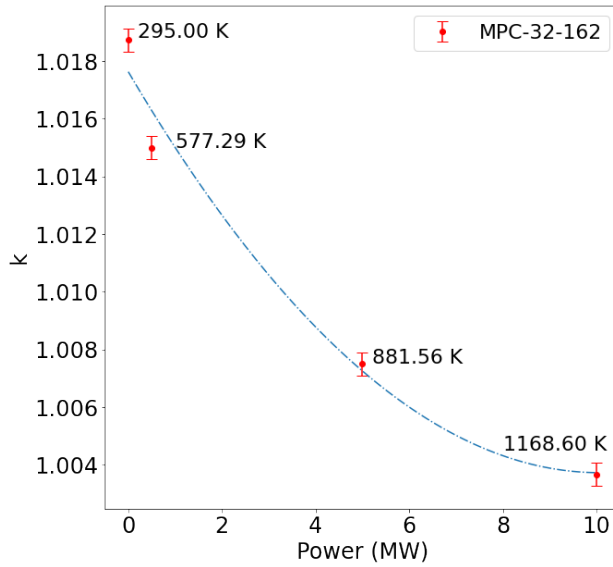


Figure 22. An example of the results from the new workflow predicting k_{eff} in a sealed DPC as a function of power. The temperatures listed on the plot represent the peak fuel temperatures in the model.

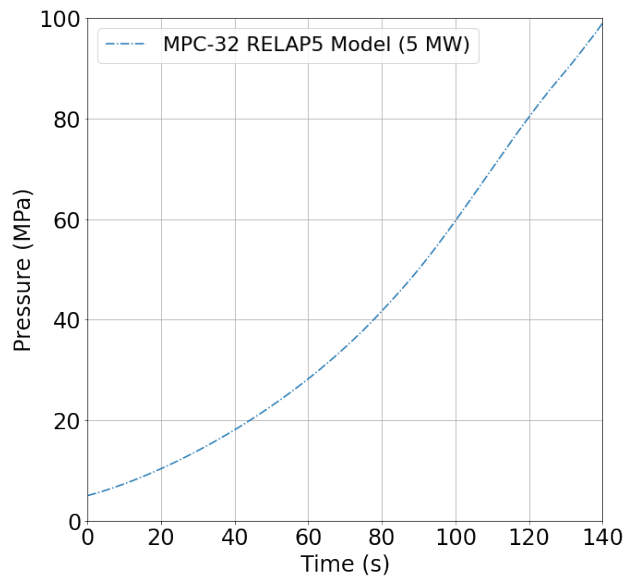


Figure 23. Pressure buildup in a sealed DPC as predicted with RELAP5-3D at a power level of 5 MW.

5. CONCLUSIONS AND FUTURE WORK

614

615 This report documents work performed to continue the development of methods for computing the
616 consequences of a critical DPC in a saturated geological repository. Four scenarios have been laid out to
617 capture the likely conditions in which a DPC could achieve criticality, along with corresponding physical
618 phenomena and modeling strategies. The methodology for computing the water level for partially filled or
619 quasi-static power level for fully filled subcooled DPCs were previously established but are summarized here
620 for completeness. The bulk of the new work presented focuses on developing a modeling strategy for the
621 most complicated case in which boiling occurs within the DPC. The ORNL research team has determined
622 that using TRACE is likely to lead to superior results compared to those predicted using RELAP5-3D.
623 Whether those results are sufficiently accurate compared to those produced by CFD codes such as STAR-
624 CCM+ remains to be determined. This model will also help inform the analysis of the final scenario in
625 which a DPC is sealed in by a saturated bentonite backfill. To support that analysis, a new python-based
626 tool was developed to enable the application of a nonhomogeneous temperature profile to the radiation
627 transport models generated by UNF-ST&DARDS and used by Shift. This tool is crucial to correctly capture
628 the Doppler broadening feedback that limits criticality in this scenario. This workflow is illustrated with
629 an example in which an MPC-32 is predicted to produce a significant amount of power, on the order of 5–
630 10 MW. It should be noted that this prediction was computed with the lower fidelity RELAP5-3D model, and
631 the results and supporting conclusions may change when the TRACE model is implemented. Nevertheless,
632 these preliminary results seem to indicate that sufficiently high pressure will be built up within the canister
633 to cause a fracture or breakthrough. Geomechanics calculations are underway with collaborators at LBNL
634 to better understand this phenomenon. If breakthrough were to occur, then boiling would commence, and
635 scenario 4 would become scenario 3, highlighting the importance of being able to accurately model boiling
636 within a DPC.

637 In the future, the authors intend to continue the lines of inquiry developed in this report. The top priority
638 will be development of a new model for simulating critical DPCs that boil prior to achieving steady-state
639 conditions. The most promising path forward to achieve this objective appears to be leveraging TRACE as
640 the primary code for capturing in-canister TH conditions. Once developed, this model can be coupled with
641 the new capability to apply temperature profiles to the radiation transport models, and an iterative approach
642 to predicting power levels for boiling (and sealed) DPCs can be demonstrated. Once a methodology for
643 modeling these final two scenarios has been developed and tested, the consequences of criticality in a DPC
644 in a saturated repository will be more comprehensively understood.

REFERENCES

645

- 646 [1] E. Hardin et al., *Investigations of dual-purpose canister direct disposal feasibility (fy14)*, tech. rep.
647 (Sandia National Lab.(SNL-NM), Albuquerque, NM (United States), 2014).
- 648 [2] M. W. Swinney et al., *Steady-state and time-dependent coupled simulations of a critical dual-purpose*
649 *canister in a saturated repository*, tech. rep. M3SF-21OR010305128, ORNL/SPR-2021/2229 (Oak
650 Ridge National Laboratory, 2021).
- 651 [3] M. W. Swinney et al., *Development of coupled simulations for critical dual-purpose canisters in a sat-*
652 *urated repository*, tech. rep. M3SF-22OR0103050812, ORNL/SPR-2022/2624 (Oak Ridge National
653 Laboratory, 2022).
- 654 [4] M. Swinney et al., “Multiphysics modeling of a critical dual-purpose canister in a saturated geological
655 repository”, *Annals of Nuclear Energy* **175** (2022).

- 656 [5] K. Banerjee et al., “Estimation of inherent safety margins in loaded commercial spent nuclear fuel
657 casks”, *Nuclear Technology* **195**, 124–142 (2016).
- 658 [6] T. M. Pandya et al., “Implementation, capabilities, and benchmarking of Shift, a massively parallel
659 Monte Carlo radiation transport code”, *Journal of Computational Physics* **308**, 239–272 (2016).
- 660 [7] I. C. Gauld, *ORIGEN: depletion module to calculate neutron activation, actinide transmutation, fis-
661 sion product generation, and radiation source terms*, tech. rep. ORNL/TM-2005/39, Version 6.1,
662 Available from Radiation Safety Information Computational Center at Oak Ridge National Labora-
663 tory as CCC-785 (Oak Ridge National Laboratory, 2011).
- 664 [8] The RELAP5-3D Code Development Team, *RELAP5-3D code manual volume I: code structure, sys-
665 tem models, and solution methods*, tech. rep. INL/MIS-15-36723, Revision 4.4 (Idaho National Lab-
666 oratory, 2018).
- 667 [9] P. C. Lichtner et al., *PFLOTRAN user manual: a massively parallel reactive flow and transport model
668 for describing surface and subsurface processes*, tech. rep. LA-UR-15-20403 (Los Alamos National
669 Laboratory, 2015).
- 670 [10] B. Rearden and M. Jessee, *SCALE code system*, tech. rep. ORNL/TM-2005/39, Version 6.2 (Oak
671 Ridge National Laboratory, 2016).
- 672 [11] G. G. Davidson et al., *Initial neutronic and thermal-hydraulic coupling for spent nuclear fuel canister*,
673 tech. rep. M3SF-19OR010305016, ORNL/SPR-2019/1144 (Oak Ridge National Laboratory, 2019).
- 674 [12] G. G. Davidson et al., “Nuclide depletion capabilities in the Shift Monte Carlo code”, *Annals of
675 Nuclear Energy* **114**, 259–276 (2018).
- 676 [13] A. E. Isotalo et al., “Flux renormalization in constant power burnup calculations”, *Annals of Nuclear
677 Energy* **96**, 148–157 (2016).
- 678 [14] C. Bertani et al., “Verification of RELAP5-3D code in natural circulation loop as function of the
679 initial water inventory”, in *Journal of physics: conference series*, 35th uit heat transfer conference,
680 Vol. 923 (2017).
- 681 [15] G. L. Messina et al., “Extremely accurate sequential verification of RELAP5-3D”, *Nuclear Science
682 and Engineering* **182**, 1–12 (2016).
- 683 [16] D. R. Rector et al., *COBRA-SFS — a thermal-hydraulic analysis computer code volume I: mathemat-
684 ical models and solution methods*, tech. rep. PNL-6049 Vol. I (Pacific Northwest National Laboratory,
685 1986).
- 686 [17] J. C. Wagner and C. V. Parks, *Recommendations on the credit for cooling time in PWR burnup credit
687 analysis*, tech. rep. NUREG/CR-6781, ORNL/TM-2001/272 (Oak Ridge National Laboratory, 2003).
- 688 [18] J. Cooper and R. Dooley, “Revised release on the iapws industrial formulation 1997 for the thermo-
689 dynamic properties of water and steam”, *The International Association for the Properties of Water
690 and Steam* **1**, 48 (2007).
- 691 [19] K. Pruess, “The tough codes—a family of simulation tools for multiphase flow and transport processes
692 in permeable media”, *Vadose zone journal* **3**, 738–746 (2004).